NANO LETTERS

2009
Vol. 9, No. 10
3592-3598

Scalable Light-Induced Metal to Semiconductor Conversion of Carbon Nanotubes

Lewis M. Gomez,† Akshay Kumar,† Yi Zhang, Koungmin Ryu, Alexander Badmaev, and Chongwu Zhou*

Department of Electrical Engineering, University of Southern California, Los Angeles, California 90089

Received June 5, 2009; Revised Manuscript Received August 14, 2009

ABSTRACT

Coexistence of metallic and semiconducting carbon nanotubes in as-grown samples sets important limits to their application in high-performance electronics. We present the metal-to-semiconductor conversion of carbon nanotubes for field-effect transistors based on both aligned nanotubes and individual nanotube devices. The conversion process is induced by light irradiation, scalable to wafer-size scales and capable of yielding improvements in the channel-current on/off ratio up to 5 orders of magnitude in nanotube-based field-effect transistors. Inactivation of metallic nanotubes in the channels was achieved as a consequence of a diameter-dependent photochemical process that led to a controlled oxidation of the nanotube sidewall and, hence, stronger localization of π-electrons. Optimization of irradiation conditions yields nearly 90% of depletable nanotube field-effect transistors.

The outstanding properties of single-walled carbon nanotubes (SWNTs) have earned them numerous applications in different technological areas.[1−3] Carbon nanotube field-effect transistors (CNTFETs) have acquired great importance due to their potential to switch on and off much faster than current silicon technologies[4−6] and the foreseen limits in the downscaling of silicon transistors.[7,8] Despite significant progress made toward integrated nanotube circuits,[4,9−11] the assembly and integration of nanotube electronics still face significant challenges due to the coexistence of metallic and semiconducting nanotubes in as-synthesized samples.

Different approaches have been followed to obtain CNTFETs containing only semiconducting nanotubes in the channels either by selective synthesis,[12−14] postsynthesis separation methods,[15−18] or postsynthesis methods to selectively etch metallic nanotubes.[19,20] Pioneering works that include the use of monochromatic light irradiation[21] and broad band light irradiation[22] to selectively etch metallic nanotubes have been reported. An alternative approach is to induce a metal-to-semiconductor transition in carbon nanotubes. Electron beam irradiation and hydrogen plasma have yielded metal-to-semiconductor conversion of SWNTs,[23−25] but the limited size of the electron beam and instability of the plasma represent limiting hurdles for scalability.

In this paper we report the use of light irradiation to induce the metal-to-semiconductor conversion of carbon nanotubes for transistors based on aligned nanotubes and individual nanotube devices. This conversion process is easy to implement and scalable to complete wafers. Aligned single-walled nanotubes were synthesized over complete quartz and sapphire wafers (Figure S1 in Supporting Information) and then transferred to a Si/SiO_2 substrate for device fabrication (Figure S2 in Supporting Information). These aligned nanotubes offer significant potential for nanotube assembly and integration,[26,27] as nanotube devices can be easily fabricated at wafer scale, as shown in Figure 1a. Figure 1b shows the photograph of an array of devices based on aligned nanotubes transferred to a 4 in. Si/SiO_2 wafer. The scanning electron microscopy (SEM) image of a typical device is shown in Figure 1b. Figure 1c illustrates the light irradiation process, where a collimated white light beam from either a xenon or halogen lamp is used to irradiate the fabricated wafer with nanotube devices for durations from 30 min to several hours. Figure 1d shows the drain current (I_{DS}) vs gate voltage (V_G) for a typical device with six aligned nanotubes before and after light irradiation with an accumulated energy of 30 kJ/cm^2. A remarkable increase in the channel current on/off ratio (I_{On}/I_{Off}) was observed from 50 before irradiation to 1.2×10^5 after irradiation. This process is highly scalable as compared to the traditional electrical breakdown approach,[19] which has to be carried out device by device. Inspection of the nanotubes after irradiation revealed no visible cut in the nanotubes (Figure S3 in Supporting Information), suggesting the increase in I_{On}/I_{Off} is due to

* Corresponding author, chongwuz@usc.edu.
† This authors contributed equally to this work.

10.1021/nl901802m CCC: $40.75
Published on Web 09/15/2009

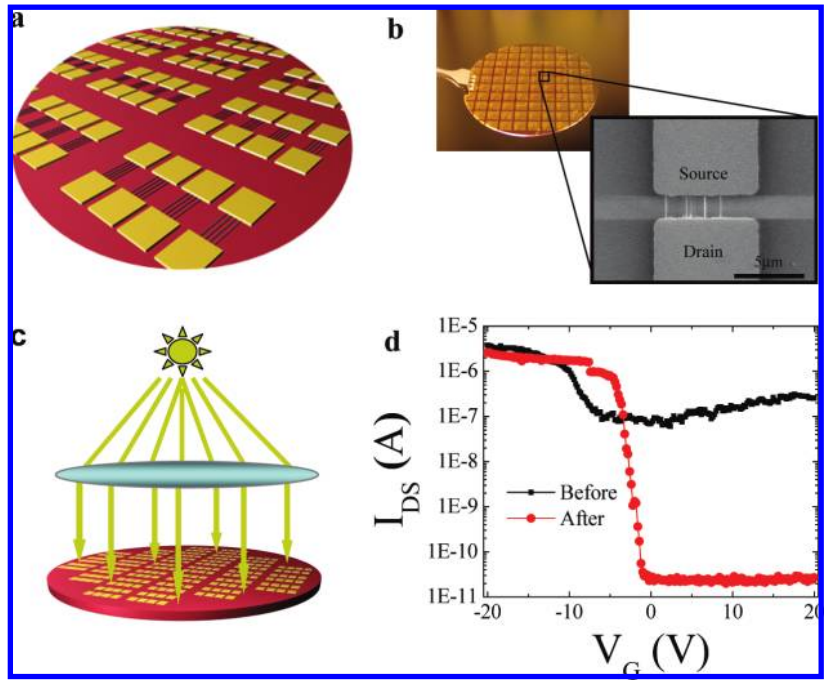

Figure 1. (a) Schematic diagram showing large arrays of field-effect transistors comprising of horizontally aligned carbon nanotubes between source and drain electrodes. (b) Photograph of a Si/SiO_2 wafer with fabricated aligned nanotube transistors. The SEM image shows a typical CNTFET in the arrays. (c) Schematic diagram illustrating the scalable light irradiation process. (d) Current vs gate voltage ($I_{DS}-V_G$) characteristics of a CNTFET device, obtained with $V_{DS} = 0.5$ V before (black trace) and after (red trace) light irradiation. The I_{On}/I_{Off} ratio increased from ~64 to ~10^5 in the nanotube transistor due to the light irradiation. Light-mediated oxidation of nanotube sidewalls leads to metal-to-semiconductor transition.

metal-to-semiconductor conversion of nanotubes in the channel.

To investigate the effect of light irradiation, we carried out electrical measurements and micro-Raman characterization for nearly 200 devices with one to five nanotubes in the channel. Parts a and b of Figure 2 show the D-band, G-band and $I_{DS}-V_G$ curves for a device with a single metallic nanotube before and after light irradiation. Analysis of the Raman spectra of this nanotube before and after irradiation reveals an increase of the Raman band intensity at 1345 cm^{-1} (D band) and a decrease of the G band intensity (1590.4 cm^{-1}), accompanied by an upshift of 5.5 cm^{-1} for the G band The ratio between the G and D Raman band intensities (I_G/I_D) is regarded as an assessment of the sp^2/sp^3 ratio in carbon nanotubes, and thus the 5-fold decrease in I_G/I_D after irradiation (Figure 2a) is attributed to an increase in the defect density due to an increase in the sp^3 nature of irradiated nanotubes.[24] It is known that rehybridization defects due to conversion of sp^2 to sp^3 sites lead to π-electrons localization that can readily open or increase the band gap of nanotubes[28] and result in the conversion of metallic to semiconductor nanotubes. The $I_{DS}-V_G$ curves of Figure 2b show that the metallic single-nanotube FET exhibited stronger gate bias dependence after light irradiation, thus indicating that an increase in the sp^3 nature of metallic nanotubes leads to metal to semiconductor conversion.[4,28−31]

To elucidate which part of the light spectrum plays the major role in the sp^2/sp^3 conversion of carbon nanotubes, we irradiated devices with ultraviolet (250−400 nm), visible (380−700 nm), and near-infrared (750−2000 nm) radiation for 1 h by using different band-pass filters between the light source and the devices. Figure 2c displays the Raman I_G/I_D before (gray bars) and after (red bars) light exposure using the full spectrum, ultraviolet, visible, and near-infrared irradiation. It is observed that both full spectrum and ultraviolet irradiation led to a decreased I_G/I_D similar in magnitude, whereas the effect of visible and near-infrared irradiation is minor and within the statistical margin of error. Further confirmation about the role of ultraviolet light is carried out by examining the Raman radial breathing mode (RBM), which is observed to be highly sensitive to light irradiation. Prolonged irradiation led to a decrease in intensity and eventual disappearance of RBM for many nanotubes (Figure 2d, inset), which can be attributed to the presence of rehybridization defects that perturb the symmetry of this vibration mode.[32] Figure 2d shows the percentage of nanotubes that remained exhibiting RBM peaks after light irradiation. Again, while the full spectrum and ultraviolet irradiation delivered similar effect (40% of examined nanotubes showed disappearance of RBM bands after irradiation), the visible and near-infrared irradiation delivered much less significant effect. Careful examination of Figure 2d inset also reveals that the nanotube with diameter $d = 1.42$ nm (174 cm^{-1}) displayed more significant decrease in RBM intensity than the nanotube with $d = 1.74$ nm (144 cm^{-1}), indicating that small-diameter nanotubes are more reactive under ultraviolet irradiation than large-diameter nanotubes.[33] Binding energies for carbon−carbon bonds with sp^2 hybridization (6.37 eV) lie well above the energy associated with photons in the UV region employed here (3.3−5.0 eV), for which the defect density increase observed upon irradiation cannot be regarded as a consequence of direct photolysis.

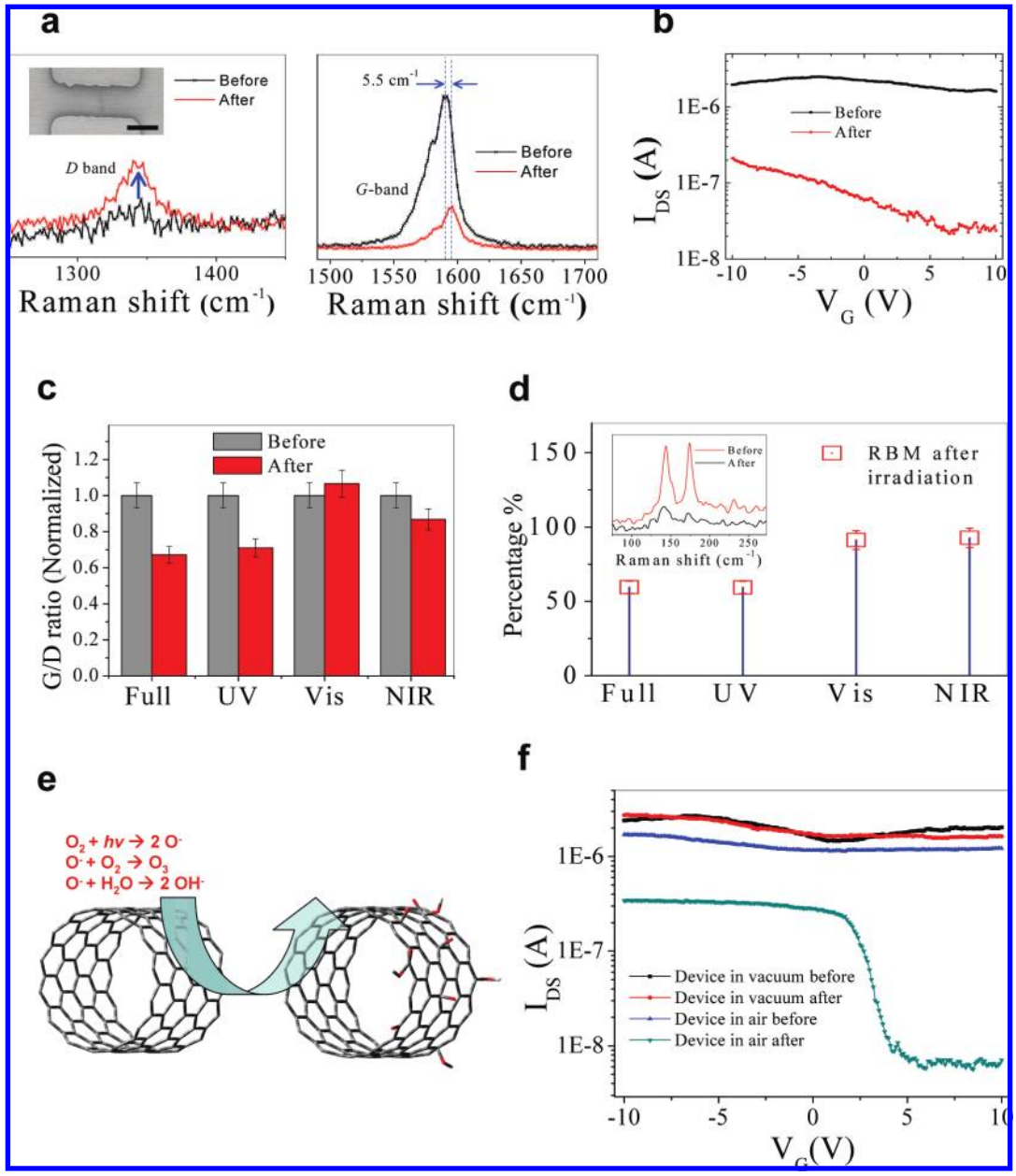

Figure 2. Light-mediated oxidation of nanotube sidewalls leads to metal-to-semiconductor transition. (a) Raman D band (left) and G band (right) of a metallic nanotube in a single-nanotube device before and after light irradiation. A 5-fold decrease in the I_G/I_D ratio shows that increased defect density on the nanotube sidewalls was achieved due to light irradiation. (b) $I_{DS}-V_G$ characteristics of the single-nanotube device shown in the inset of (a), before and after light irradiation. The I_{On}/I_{Off} improved from 1.6 to 10.5, indicating metal to semiconductor transition. (c) Comparison between the G/D ratios of nanotubes before and after 1 h of irradiation with the full spectrum, ultraviolet, (250−400 nm), visible (380−700 nm), and near-infrared (750−2000 nm) radiation. (d) Percentage of nanotubes exhibiting Raman RBM signal after light irradiation using the same irradiation conditions as part c. The inset shows that the decrease of RBM intensity was more significant for the small-diameter nanotube than for larger nanotubes. (e) Schematic showing light-induced oxidation of the nanotube sidewalls. Possible chemical groups were introduced on the nanotube sidewalls upon sp^2-sp^3 rehybridization by light-induced oxidation. (f) Comparison of typical $I_{DS}-V_G$ characteristics of two CNTFETs before and after irradiation in air and in vacuum. The device irradiated in air became fully depletable, showing an improvement in I_{On}/I_{Off} from 1.7 to 100, while the device irradiated in vacuum exhibited virtually no change in its transistor characteristics.

We attribute the observed metal-to-semiconductor conversion to UV-assisted photo-oxidation of nanotubes in oxygen-containing environment. Increased absorption in the region 3100−3600 cm^{-1} was found on control nanotube samples after light irradiation using mid-FTIR spectroscopy, indicating increased presence of oxygen functionalities in irradiated nanotubes mainly in the form of hydroxylic groups (see Supporting Information). UV-irradiated oxygen forms oxygen radicals and ozone, which are strong gas-phase oxidants.[34,35] Figure 2e shows a schematic of carbon nanotube oxidation due to light irradiation in air. The radical-driven reactions can be triggered by UV radiation and readily contribute to the surface functionalization of nanotubes with oxygen-containing groups. Oxidation of nanotube sidewall is also consistent with the upshift seen in the Raman G band (Figure 2a), which can be related to interaction between

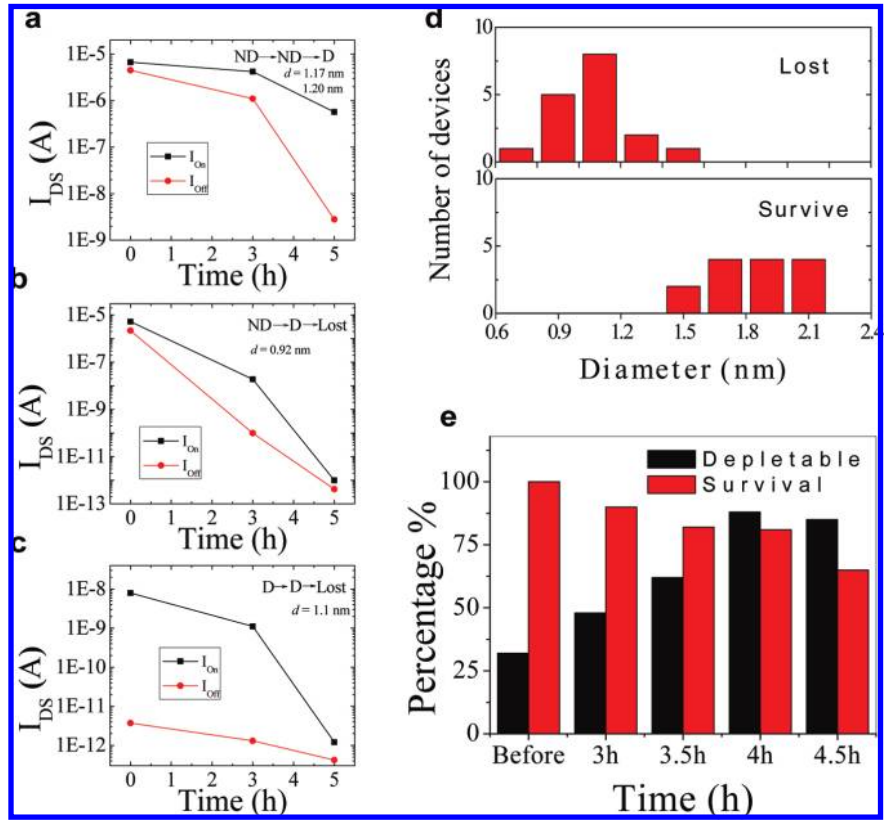

Figure 3. Influence of the irradiation time and nanotube diameter on the metal-to-semiconductor conversion observed in CNTFETs. (a, b, and c) I_{On} and I_{Off} of single- and few-nanotube CNTFETs showing different evolutions under timed light irradiation (V_{ds} = 100 mV). (d) Histogram of CNTFETs that lost electrical conduction or survived after 6 h of light irradiation plotted versus the nanotube diameter. Clear diameter dependence was observed. (e) Percentage of CNTFETs that survived (red) and showed depletable behavior (black) for different light irradiation durations. The best yield was found after 4 h of exposure, when the percentage of depletable devices increased from 32% to 88% while keeping a survival ratio near 81%.

electron-withdrawing oxygen functionalities and the π-electron system on the nanotube sidewall.[36,37] Further confirmation of the role of oxygen in the photoassisted metal-to-semiconductor conversion was obtained by comparing the effects of light irradiation on nanotube transistors in air and in vacuum (3×10^{-5} Torr). Typical examples are shown in Figure 2f. The device exposed to light irradiation in vacuum (black and red curves) exhibited little change in the on-state current and the I_{On}/I_{Off}. In contrast, the device exposed to irradiation in air (blue and green curves) displayed an increase in I_{On}/I_{Off} and a drop in the on-state current. This unambiguously confirms the important role of oxygen for the light-assisted metal-to-semiconductor conversion of nanotubes.

To further elucidate the underlying mechanism and to optimize the yield of depletable transistors by light irradiation, we have carried out detailed experiments on 38 working devices with single or a few nanotubes with varying irradiation time. A "lost" device is defined as a device with $I_{On} < 100$ pA at $V_{ds} = 0.1$ V. In contrast, devices with $I_{On} \geq 100$ pA at $V_{ds} = 0.1$ V are categorized as survived devices, among which depletable devices are defined as having $I_{On}/I_{Off} \geq 10$ and nondepletable devices are those with $I_{On}/I_{Off} < 10$. AFM was performed to obtain the diameter of each nanotube. Light-induced metal-to-semiconductor conversion was found to be stable and irreversible at ambient conditions, in contrast to the behavior observed by Ajayan.[38] CNTFETs were grouped into three categories according to their transport characteristics at time = 0, 3 h, and 5 h under exposure: (i) CNTFETs that showed metallic behavior but were converted into semiconducting and remained depletable throughout the irradiation process (Figure 3a, nondepletable to nondepletable to depletable [ND → ND → D]); (ii) nondepletable CNTFETs that first became depletable and then lost electrical conduction upon continued irradiation (Figure 3b, nondepletable to depletable to lost [ND → D → Lost]); and (iii) CNTFETs that were depletable before irradiation and then lost electrical conduction after continued light irradiation (Figure 3c, depletable to depletable to lost [D → D → Lost]). The CNTFET in Figure 3a has two nanotubes with d = 1.17 and 1.20 nm connecting source and drain electrodes. I_{On}/I_{Off} for this device changed as 1.5 → 3.8 → 203 for 0, 3, and 5 h of light exposure, respectively. On the other hand, the nanotube in the single-nanotube device shown in Figure 3b has a diameter of 0.92 nm and its I_{On}/I_{Off} changed as 2.4 → 191 for 0 and 3 h, respectively. Radial tension possessed by small-diameter carbon nanotubes decrease their stability and increase their reactivity compared to those with larger diameters,[39] which explains why light irradiation for the device in Figure 3b would first make it depletable but later too resistive for charge transport. Furthermore, I_{On}/I_{Off} for the single nanotube CNTFET in

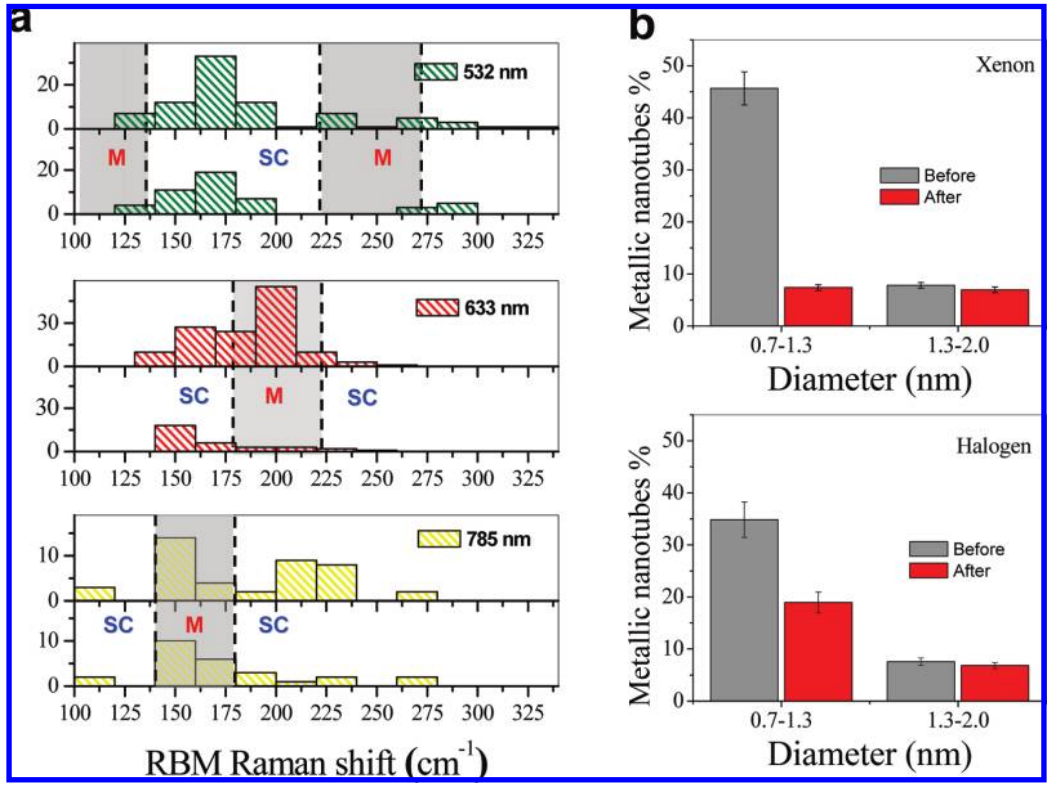

Figure 4. (a) Stacked histograms showing the number of nanotubes exhibiting RBM vs the RBM frequency, before and after light irradiation, as measured with three excitation lines (532, 633, and 785 nm). Frequency regions characteristic for metal or semiconductor nanotubes are highlighted based on Kataura's plot. Comparison of the histograms obtained before and after irradiation for each laser shows a predominant light-induced oxidation of small-diameter nanotubes (large RBM frequency). (b) Percentage of metallic nanotubes in as-grown samples before (gray columns) and after (red columns) light exposure using xenon (upper panel) and halogen (lower panel) lamps. Nanotubes were grouped into two categories based on their diameter: small-diameter (0.7−1.3 nm) and large-diameter (1.4−2.0 nm) nanotubes. A substantial decrease in the percentage of small-diameter metallic nanotubes found after light irradiation, for both light sources employed, indicates their preferential oxidation over semiconducting small-diameter nanotubes. Contrarily, the percentage of large-diameter metallic nanotubes was largely unaffected by light, indicating the preferential oxidation (metal over semiconductor) is more effective for small-diameter nanotubes.

Figure 3c ($d = 1.1$ nm) changed as 2135 → 846 upon light irradiation for 0 and 3 h, respectively. Comparison between Figure 3a and Figure 3b confirms that small-diameter nanotubes are more reactive, as electrical conduction was lost in Figure 3b, but persisted in Figure 3a after 5 h of exposure.

The effect of prolonged light exposure on a chip with 38 working CNTFETs is shown in Figure 3d. Devices with nanotube diameters ranging from 0.6 to ∼1.3 nm became nearly open circuits, while those with nanotube diameters larger than 1.4 nm in general survived light exposure. After nearly 6 h of irradiation, most (90%) of the surviving devices (20 CNTFETs) were depletable and exhibited clear semiconducting behavior. Similar diameter dependence has also been observed for nanotube devices exposed to H_2 plasma[24,25] and CH_4 plasma[22] due to the higher curvature of small-diameter nanotubes that makes them more reactive than their large-diameter counterparts. As demonstrated above, prolonged light-assisted oxidation of the nanotube sidewall may lead to highly resistive devices. Thus, it is important to find the exposure time that best optimizes the trade-off between depletable and surviving devices. Figure 3e shows the change in the percentage of depletable (black) and surviving (red) CNTFETs from a chip with 31 working devices, as a function of light exposure time with a power density of 2.2 W/cm^2. The best yield was obtained after 4 h of light exposure, which offered ∼88% depletable devices and a survival rate of ∼81%. This yield is typical for devices with five nanotubes or less in the channel. However, the effect of the metal to semiconductor conversion in I_{On}/I_{Off} is generally less pronounced in devices with a larger number of nanotubes, which can be improved by using CNTFETs with optimum and narrower diameter distribution.

Now that the diameter dependence has been elucidated, we have carried out micro-Raman measurements to ascertain whether light irradiation provides selectivity between metal and semiconductor tubes of similar diameters (Figure 4). Covalent functionalization of a SWNT sidewall is accompanied by a decrease in the RBM intensity below the noise level (disappearance of RBM bands).[40,41] For complete characterization, we have carried out micro-Raman spectroscopy with three different excitation lines (532, 633, and 785 nm). Figure 4A shows plots of the number of nanotubes exhibiting RBM v.s. the RBM frequency before and after irradiation as measured with all three excitation lines. The frequencies characteristic for metal and semiconductor nanotubes are highlighted based on Kataura's plot. Detailed analysis of the data shown in Figure 4a, for all lasers

employed, reveals a diameter-dependent decrease of nanotubes showing RBM, which correlates to the increased sp^3 character of nanotubes upon light irradiation. By comparing the histograms in Figure 4a before and after light irradiation, one can clearly see that predominantly small-diameter nanotubes (with large RBM frequency) underwent disappearance of RBM bands, which is consistent with the diameter dependence shown in Figure 3. Interestingly, most metallic nanotubes with M_{11} band gaps in resonance with visible laser wavelengths 532 nm (2.32 eV) and 633 nm (1.96 eV) have diameters lower than ~1.3 nm, which means they are more likely to be oxidized by light irradiation. NIR laser energy with wavelength of 785 nm (1.58 eV) is, in contrast, in good resonance with S_{11} and S_{22} band gaps of semiconducting nanotubes with diameters lower than 1.3−1.4 nm and metallic nanotubes with larger diameters. Results shown in Figure 4a further confirm, for all lasers employed, a well marked diameter-dependent oxidation of nanotubes.

We irradiated as-grown nanotubes with the full spectrum of xenon and halogen light sources. Figure 4b shows the percentage of metallic nanotubes in the samples, before and after irradiation. Nanotubes were grouped into two categories based on their diameter (0.7−1.3 nm and 1.4−2.0 nm). Importantly, we observed for both light sources a marked preferential oxidation of metallic nanotubes with diameters between 0.7 and 1.3 nm over their semiconducting counterparts, with a decrease in the percentage of metallic nanotubes from 45 to 7% and 35 to 18% for xenon and halogen irradiation, respectively. The difference observed in the effect of xenon and halogen light sources over the oxidation of small-diameter nanotubes can be related to the higher intensity of UV photons of the former.[42] On the other hand, there was no significant difference between the oxidation of large-diameter metallic and semiconducting nanotubes in the diameter range of 1.4−2.0 nm. This means that higher radial tension, added to the presence of free electrons on the conduction band of small-diameter metallic nanotubes, makes them more reactive, upon light-induced oxidation, than semiconducting nanotubes of similar diameters, for which appropriate irradiation times as well as narrow diameter distribution are key to obtain semiconducting CNTFET arrays by light irradiation.

Light irradiation of nanotubes constitutes a breakthrough scalable process for nanotube-based electronic devices via a defect-assisted metal-to-semiconductor conversion stimulated by light-induced oxidation. This process was found to be diameter dependent and faster in small-diameter metallic nanotubes. I_{on}/I_{off} improvements obtained in CNTFETs were typically in the range of 10^2 up to 10^5 and can be easily scaled and integrated as a customizable technology over larger-diameter wafers. The approach presented in this work offers clear advantages over conventional processes to eliminate metallic nanotubes from CNTFETs and constitutes a significant advance toward large scale fabrication of carbon nanotube based electronic devices.

Acknowledgment. We acknowledge financial support from the SRC FCRP FENA Center, and the National Science Foundation (CCF-0726815 and CCF-0702204). We thank professor Stephen Cronin for access to micro Raman system. The authors also thank S. Jonas and V. Tung for IR measurements.

Supporting Information Available: Additional information regarding wafer scale synthesis of aligned nanotubes on quartz and sapphire, transfer of aligned nanotubes and device fabrication, effect of light on morphology and transfer characteristics of a metallic single nanotube CNT-FET, and FTIR spectroscopy of light-irradiated carbon nanotubes. This material is available free of charge via the Internet at http://pubs.acs.org.

References

(1) Thostenson, E. T.; Ren, Z.; Chou, T.-W. Advances in the science and technology of carbon nanotubes and their composites: a review. *Compos. Sci. Technol.* **2001**, *61*, 1899–1912.
(2) Avouris, P.; Chen, Z.; Perebeinos, V. Carbon-based electronics. *Nat. Nanotechnol.* **2007**, *2*, 605–615.
(3) Mahar, B.; Laslau, C. Development of Carbon Nanotube-Based Sensors—A Review. *IEEE Sens. J.* **2007**, *7*, 19.
(4) Bachtold, A.; Hadley, P.; Nakanishi, T.; Dekker, C. Logic Circuits with Carbon Nanotube Transistors. *Science* **2001**, *294*, 1317–1320.
(5) Javey, A.; Guo, J.; Wang, Q.; Lundstrom, M.; Dai, H. Ballistic carbon nanotube field-effect transistors. *Nature* **2003**, *424*, 654–657.
(6) Dulrkop, T.; Getty, S. A.; Cobas, E.; Fuhrer, M. S. Extraordinary Mobility in Semiconducting Carbon Nanotubes. *Nano Lett.* **2004**, *4*, 35–39.
(7) Avouris, P.; et al. Carbon nanotubes: nanomechanics, manipulation, and electronic devices. *Appl. Surf. Sci.* **1999**, *141*, 201–209.
(8) Bohr, M. T. Nanotechnology Goals and Challenges for Electronic Applications. *IEEE Trans. Nanotechnol.* **2001**, *1*, 56–62.
(9) Javey, A.; Wang, Q.; Ural, A.; Li, Y.; Dai, H. Carbon Nanotube Transistor Arrays for Multistage Complementary Logic and Ring Oscillators. *Nano Lett.* **2002**, *2*, 929–932.
(10) Chen, Z.; An Integrated Logic Circuit Assembled on a Single Carbon Nanotube *Science* **2006**, *311*, 1735.
(11) Cao, Q.; et al. Medium-scale carbon nanotube thin-film integrated circuits on flexible plastic substrates. *Nature* **2008**, *454*, 495500..
(12) Bachilo, S. M.; et al. Narrow (n,m)-Distribution of Single-Walled Carbon Nanotubes Grown Using a Solid Supported Catalyst. *J. Am. Chem. Soc.* **2003**, *125*, 11186–11187.
(13) Li, Y.; et al. Preferential Growth of Semiconducting Single-Walled Carbon Nanotubes by a Plasma Enhanced CVD Method. *Nano Lett.* **2004**, *4*, 317–321.
(14) Joselevich, E.; Lieber, C. M. Vectorial Growth of Metallic and Semiconducting Single-Wall Carbon Nanotubes. *Nano Lett.* **2002**, *2*, 1137–1141.
(15) Chen, Z.; et al. Bulk Separative Enrichment in Metallic or Semiconducting Single-Walled Carbon Nanotubes. *Nano Lett.* **2003**, *3*, 1245–1249.
(16) Arnold, M. S.; Green, A. A.; Hulvat, J. F.; Stupp, S. I.; Hersam, M. C. Sorting carbon nanotubes by electronic structure using density differentiation. *Nat. Nanotechnol.* **2006**, *1*, 6.
(17) Chen, F.; Wang, B.; Chen, Y.; Li, L.-J. Toward the Extraction of Single Species of Single-Walled Carbon Nanotubes Using Fluorene-Based Polymers. *Nano Lett.* **2007**, *7*, 3013–3017.
(18) Nish, A.; Hwang, J.-Y.; Doig, J.; Nicholas, R. J. Highly selective dispersion of single-walled carbon nanotubes using aromatic polymers. *Nat. Nanotechnol.* **2007**, *2*, 640–646.
(19) Collins, P. G.; Arnold, M. S.; Avouris, P. Engineering Carbon Nanotubes and Nanotube Circuits Using Electrical Breakdown. *Science* **2001**, *292*, 706–709.
(20) Zhang, G.; et al. Selective Etching of Metallic Carbon Nanotubes by Gas-Phase Reaction. *Science* **2006**, *314*, 974–977.
(21) Huang, H.; Maruyama, R.; Noda, K.; Kajiura, H.; Kadono, K. Preferential Destruction of Metallic Single-Walled Carbon Nanotubes by Laser Irradiation. *J. Phys. Chem. B* **2006**, *110*, 7316–7320.
(22) Zhang, Y.; Zhang, Y.; Xian, X.; Zhang, J.; Liu, Z. Sorting out Semiconducting Single-Walled Carbon Nanotube Arrays by Preferential Destruction of Metallic Tubes Using Xenon-Lamp Irradiation. *J. Phys. Chem. C* **2008**, *112*, 8.
(23) Chen, B.-H.; et al. Novel Method of Converting Metallic-Type Carbon Nanotubes to Semiconducting-Type Carbon Nanotube Field-Effect Transistors. *Jpn. J. Appl. Phys.* **2006**, *45*, 3680–3685.

(24) Zhang, G.; et al. Hydrogenation and Hydrocarbonation and Etching of Single-Walled Carbon Nanotubes. *J. Am. Chem. Soc.* **2006**, *128*, 6026–6027.
(25) Zheng, G.; et al. Transition of Single-Walled Carbon Nanotubes from Metallic to Semiconducting in Field-Effect Transistors by Hydrogen Plasma Treatment. *Nano Lett.* **2007**, *7*, 1622–1627.
(26) Han, S.; Liu, X.; Zhou, C. Template-Free Directional Growth of Single-Walled Carbon Nanotubes on a- and r-Plane Sapphire. *J. Am. Chem. Soc.* **2005**, *127*, 5294–5295.
(27) Liu, X.; Han, S.; Zhou, C. Novel Nanotube-on-Insulator (NOI) Approach toward Single-Walled Carbon Nanotube Devices. *Nano Lett.* **2006**, *6*, 34–39.
(28) Park, K. A.; Seo, K.; Leeand, Y. H. Adsorption of Atomic Hydrogen on Single-Walled Carbon Nanotubes. *J. Phys. Chem. B* **2005**, *109*, 8967–8972.
(29) Derycke, V.; Martel, R.; Appenzeller, J.; Avouris, P. Carbon Nanotube Inter- and Intramolecular Logic Gates. *Nano Lett.* **2001**, *1*, 453–456.
(30) Zhou, W.; et al. Structural characterization and diameter-dependent oxidative stability of single wall carbon nanotubes synthesized by the catalytic decomposition of CO. *Chem. Phys. Lett.* **2001**, *350*, 6–14.
(31) Park, S.; Srivastava, D.; Cho, K. Generalized Chemical Reactivity of Curved Surfaces: Carbon Nanotubes. *Nano Lett.* **2003**, *3*, 1273–1277.
(32) Gomez De Arco, L.; Lei, B.; Cronin, S.; Zhou, C. Resonant micro-Raman spectroscopy of aligned single-walled carbon nanotubes on a-plane sapphire. *Appl. Phys. Lett.* **2008**, *93*, 123112.1123112.3.
(33) Chan, S.-P.; Chen, G.; Gong, X. G.; Liu, Z.-F. Oxidation of Carbon Nanotubes by Singlet O_2. *Phys. Rev. Lett.* **2003**, *90*, 4.
(34) Zellner, R. *Global Aspects of Atmospheric Chemistry*; Baumgartel, H., Grunbein, W., Hensel, F., Eds.; Springer: New York, 1999.
(35) Tedetti, M.; et al. Hydroxyl radical-induced photochemical formation of dicarboxylic acids from unsaturated fatty acid (oleic acid) in aqueous solution. *J. Photochem. Photobiol., A* **2007**, *188*, 4.
(36) Kim, U. J.; Furtado, C. A.; Liu, X.; CHEN, G.; Eklund, P. C. Raman and IR Spectroscopy of Chemically Processed Single-Walled Carbon Nanotubes. *J. Am. Chem. Soc.* **2005**, *127*, 15437–15445.
(37) Chen, G.; et al. Chemically Doped Double-Walled Carbon Nanotubes: Cylindrical Molecular Capacitors. *Phys. Rev. Lett.* **2003**, *90*, 257403-1–257403-4.
(38) Vijayaraghavan, A.; et al. Metal-Semiconductor Transition in Single-Walled Carbon Nanotubes Induced by Low-Energy Electron Irradiation. *Nano Lett.* **2005**, *5*, 1575–1579.
(39) Seo, K.; et al. Chirality- and Diameter-Dependent Reactivity of NO_2 on Carbon Nanotube Walls. *J. Am. Chem. Soc.* **2005**, *127*, 15724–15729.
(40) Wang, C.; et al. Electronically Selective Chemical Functionalization of Carbon Nanotubes: Correlation between Raman Spectral and Electrical Responses. *J. Am. Chem. Soc.* **2005**, *127*, 11460–11468.
(41) Buffa, F.; Hu, H.; Resasco, D. E. Side-Wall Functionalization of Single-Walled Carbon Nanotubes with 4-Hydroxymethylaniline Followed by Polymerization of -Caprolactone. *Macromolecules* **2005**, *38*, 8258–8263.
(42) Spectral irradiance of xenon and halogen lamps was provided by Newport Co.

NL901802M